Syntheses, and Structural, Magnetic, and Redox Properties of Multinuclear Copper Catecholates†

Eric Gojon and Jean-Marie Latour*
DRF/LCH (UA 1194), CENG, 85X 38041 Grenoble Cedex, France
Stephen J. Greaves, David C. Povey, Vijayalakshmi Ramdas, and Gallienus W. Smith
Department of Chemistry, University of Surrey, Guildford GU2 5XH

Interaction of copper salts with a ligand (H_2L^1) obtained by condensation of 3,4-dihydroxybenzaldehyde with 2-aminomethylpyridine allows one to isolate a nitrato $[\{Cu(HL^1)(NO_3)\}_4]$, (**1**), a chloro $[\{Cu(HL^1)Cl\}_2]$, (**2**), and an acetato $[\{CuL^1(CH_3CO_2)\}_4]$, (**3**), derivative. The acetato derivative $[\{Cu_2L^2(CH_3CO_2)_2\}_2]$, (**4**), of a ligand ($H_2L^2$) prepared from 2-(2′-aminoethyl)pyridine has been isolated in the crystalline state and its structure solved by *X*-ray diffractometry. It crystallizes in the space group $P\bar{1}$, with a = 8.365(2), b = 9.667(1), c = 12.556(1) Å, α = 98.40(2), β = 103.97(2), and γ = 94.26(2)°. The tetranuclear arrangement results from dimerization of the dinuclear unit comprising one copper atom in the chelated site (O_2) and one in the lateral site (N_2O) through the external catechol oxygen. Complex (**1**) crystallizes in the space group $P2_1/n$, with a = 20.47(5), b = 21.27(5), c = 14.31(7) Å, and β = 93.93(7)°. It is tetranuclear in the solid state and adopts a distorted cubane structure with a Cu_4O_4 core, the four copper atoms being bridged by the internal catechol oxygens of the ligand molecules. The magnetic properties of both compounds are interpreted with the magnetic orbital concept. Electrochemical studies revealed that, in (**1**), both the metal and the ligand are electroactive.

In the recent past the co-ordination chemistry of catechols has grown steadily.[1] The reasons for this increased interest are two-fold. First, the importance of the oxidative transformations of catechols for synthetic procedures has been recognized.[2] Secondly, biochemical studies have revealed the involvement of various catechol derivatives in a large number of natural processes. Actually, catechols can function as electron donors,[3] complexing agents in carrier proteins,[4] and substrates, intermediates or products of oxidation reactions.[5] In most of these processes the catechols are found to interact with transition-metal ions, iron and copper mainly, and to act through their redox as well as their complexing properties.

Numerous solution studies have demonstrated the high affinity of catecholates for copper(II).[6] In particular, Sigel and co-workers[7] have shown the exceptional stability of copper complexes in which a catecholate is associated with an aromatic diamine, (**A**). In the past decade, several copper catecholates have been isolated,[2,8–18] in several instances[2,8,11,12] with the aim of examining their oxidative transformations. From the early work on, the catecholate was assumed to chelate the copper ion, (**A**); however, this bonding mode has been confirmed only recently by *X*-ray structural determinations. Thompson and Calabrese[14] and Buchanan *et al.*[16] reported the structures of copper complexes of 3,5-di-t-butylbenzosemiquinone and 3,5-di-t-butylcatechol, respectively, where the chelating catechol derivative is associated with a bipyridyl coligand. A notable exception has been described by Karlin *et al.*[15] who prepared the tetrachlorocatecholate adduct of a μ-phenoxo-dicopper complex. In this compound, the catecholate is no longer chelating but bridges the two copper atoms, as in (**B**).

As part of a project aimed at synthesizing multicopper complexes of redox-active ligands,[17,18] we investigated the possibility of obtaining copper catecholates in which the catechol is not chelating. Two advantages are expected from this unsymmetrical bonding mode. First, the second (or both) oxygen(s) can be used to complex a second metal ion. Secondly, an equatorial co-ordination site of the metal is left open to exogenous ligand bonding. In order to divert the catechol from its usual chelating bonding mode, we introduced complexing side arms bearing nitrogen donors onto *ortho* positions of pyrocatechol. In this report, we describe the synthesis and the physicochemical properties of a series of copper catecholates of the ligands H_2L^1 and H_2L^2. We present the structure determinations of a linear tetranuclear acetato complex of H_2L^2 and of the nitrate derivative of H_2L^1 which is also tetranuclear but possesses a distorted cubane geometry. An early account[17] of this work has been published as well as a report[18] of the properties of a related pentacopper cluster of a catechol bearing two complexing side arms.

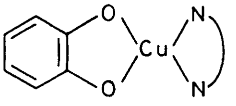

(**A**)

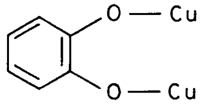

(**B**)

Results and Discussion

Structural Studies.—Figure 1 shows the structure of compound (**4**), and atomic co-ordinates and bond lengths and angles are collected in Tables 1 and 2. The molecule results from the dimerization of two dinuclear units which are built around a catechol ligand. Both oxygen atoms of the catechol are deprotonated and available for co-ordination. Each ligand is then able to bind two copper ions: one [Cu(1)] within the lateral N_2O site and the second [Cu(2)] in the chelated site. The two copper ions are thus bridged by one ligand oxygen, O(2); two

---

† *Supplementary data available:* see Instructions for Authors, *J. Chem. Soc., Dalton Trans.*, 1990, Issue 1, pp. xix–xxii.

Table 1. Atomic positional parameters (× 10^4) with estimated standard deviations (e.s.d.s) for compound (**4**)

Atom	*x*	*y*	*z*	Atom	*x*	*y*	*z*
Cu(1)	0.368 21(8)	0.636 71(6)	0.681 79(5)	C(5)	0.225 6(7)	0.549 5(6)	0.413 9(4)
Cu(2)	0.518 99(8)	0.909 48(6)	0.591 29(5)	C(6)	0.317 2(6)	0.680 4(5)	0.456 5(4)
O(1)	0.392 3(5)	0.911 6(4)	0.440 8(3)	C(7)	0.231 4(8)	0.436 0(6)	0.478 9(5)
O(2)	0.424 8(4)	0.709 7(4)	0.558 6(3)	C(8)	0.279 8(9)	0.319 9(6)	0.633 0(5)
O(3)	0.592 0(5)	0.724 1(4)	0.788 4(3)	C(9)	0.399 9(8)	0.338 6(6)	0.746 1(5)
O(4)	0.694 7(5)	0.900 3(4)	0.719 0(3)	C(10)	0.345 0(7)	0.431 8(6)	0.832 8(5)
O(5)	0.188 4(5)	0.776 3(4)	0.683 9(4)	C(11)	0.321 2(8)	0.388 6(6)	0.928 9(5)
O(6)	0.341 0(6)	0.975 7(5)	0.684 5(4)	C(12)	0.272 0(8)	0.480 3(7)	1.006 4(5)
O(7)	0.500	0.000	0.000	C(13)	0.248 3(8)	0.613 3(7)	0.986 4(5)
N(1)	0.288 2(6)	0.449 0(4)	0.583 2(4)	C(14)	0.271 7(8)	0.651 5(6)	0.889 6(5)
N(2)	0.321 3(6)	0.564 5(4)	0.814 7(4)	C(15)	0.699 2(7)	0.820 4(6)	0.789 3(5)
C(1)	0.301 0(7)	0.788 0(5)	0.391 6(4)	C(16)	0.853(1)	0.848 5(8)	0.885 0(6)
C(2)	0.198 6(7)	0.762 3(6)	0.284 4(4)	C(17)	0.207 4(8)	0.904 9(6)	0.677 9(5)
C(3)	0.110 8(7)	0.630 4(6)	0.242 5(5)	C(18)	0.058(1)	0.973 7(9)	0.660(1)
C(4)	0.123 2(7)	0.525 4(6)	0.305 2(5)				

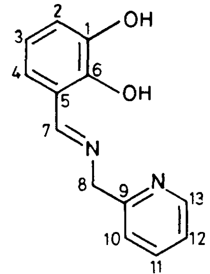

H_2L^1

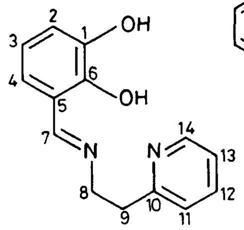

H_2L^2

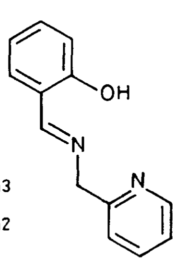

HL^3

(**1**) $[\{Cu(HL^1)(NO_3)\}_4]$
(**2**) $[\{Cu(HL^1)Cl\}_2]$
(**3**) $[\{Cu_2L^1(CH_3CO_2)_2\}_2]$
(**4**) $[\{Cu_2L^2(CH_3CO_2)_2\}_2]$

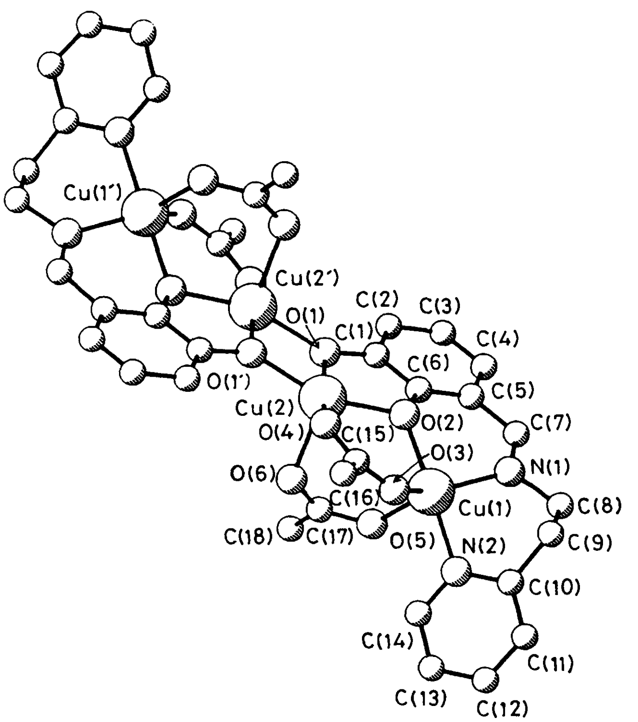

Figure 1. Structure of compound (**4**)

Table 2. Bond lengths (Å) and angles (°) with e.s.d.s for compound (**4**)

Cu(1)–O(2)	1.933(3)	N(1)–C(7)	1.265(7)
Cu(1)–O(3)	2.058(4)	N(1)–C(8)	1.480(7)
Cu(1)–O(5)	2.096(4)	N(2)–C(10)	1.355(6)
Cu(1)–N(1)	2.009(4)	N(2)–C(14)	1.332(7)
Cu(1)–N(2)	2.010(4)	C(1)–C(2)	1.386(7)
Cu(2)–O(1)	1.934(4)	C(1)–C(6)	1.407(7)
Cu(2)–O(2)	1.976(3)	C(2)–C(3)	1.386(8)
Cu(2)–O(4)	1.913(4)	C(3)–C(4)	1.368(8)
Cu(2)–O(6)	2.181(5)	C(4)–C(5)	1.401(8)
Cu(2)–O(1′)	1.965(4)	C(5)–C(6)	1.390(7)
O(1)–C(1)	1.346(6)	C(5)–C(7)	1.458(8)
O(2)–C(6)	1.353(6)	C(8)–C(9)	1.506(9)
O(3)–C(15)	1.240(6)	C(9)–C(10)	1.491(8)
O(4)–C(15)	1.251(6)	C(10)–C(11)	1.387(8)
O(5)–C(17)	1.257(7)	C(11)–C(12)	1.378(9)
O(6)–C(17)	1.245(7)	C(12)–C(13)	1.365(9)
C(15)–C(16)	1.511(9)	C(13)–C(14)	1.373(8)
C(17)–C(18)	1.443(11)		
O(2)–Cu(1)–O(3)	91.7(2)	O(1)–C(1)–C(2)	124.5(5)
O(2)–Cu(1)–O(5)	90.4(2)	O(1)–C(1)–C(6)	115.3(4)
O(2)–Cu(1)–N(1)	89.6(2)	C(2)–C(1)–C(6)	120.2(5)
O(2)–Cu(1)–N(2)	177.1(2)	C(1)–C(2)–C(3)	119.4(5)
O(3)–Cu(1)–O(5)	110.7(2)	C(2)–C(3)–C(4)	121.1(5)
O(3)–Cu(1)–N(1)	133.9(2)	C(3)–C(4)–C(5)	120.3(5)
O(3)–Cu(1)–N(2)	85.4(2)	C(4)–C(5)–C(6)	119.4(5)
O(5)–Cu(1)–N(1)	115.4(2)	C(4)–C(5)–C(7)	118.5(5)
O(5)–Cu(1)–N(2)	90.9(2)	C(6)–C(5)–C(7)	122.1(5)
N(1)–Cu(1)–N(2)	92.2(2)	O(2)–C(6)–C(1)	117.5(4)
O(1)–Cu(2)–O(2)	83.6(1)	O(2)–C(6)–C(5)	122.9(5)
O(1)–Cu(2)–O(4)	163.4(2)	C(1)–C(6)–C(5)	119.6(5)
O(1)–Cu(2)–O(6)	100.6(2)	N(1)–C(7)–C(5)	125.8(5)
O(2)–Cu(2)–O(4)	98.2(2)	N(1)–C(8)–C(9)	111.0(5)
O(2)–Cu(2)–O(6)	93.7(2)	C(8)–C(9)–C(10)	112.6(5)
O(4)–Cu(2)–O(6)	95.8(2)	N(2)–C(10)–C(9)	116.7(5)
Cu(1)–O(2)–Cu(2)	115.3(2)	N(2)–C(10)–C(11)	120.4(5)

acetates complete the bridging network. With such an arrangement of the ligand the copper atom in the chelated site would be bound to only four oxygen atoms. This is insufficient for a copper(II) ion which usually prefers five-co-ordination. Thus, a fifth ligand is provided by a catechol oxygen from another binuclear unit. The need for an additional ligand is the probable driving force for the dimerization. The two binuclear units are related by a centre of symmetry located at the centre of the Cu(2)O(1)Cu(2′)O(1′) parallelogram. The geometries of the two distinct copper sites are quite different. The environment

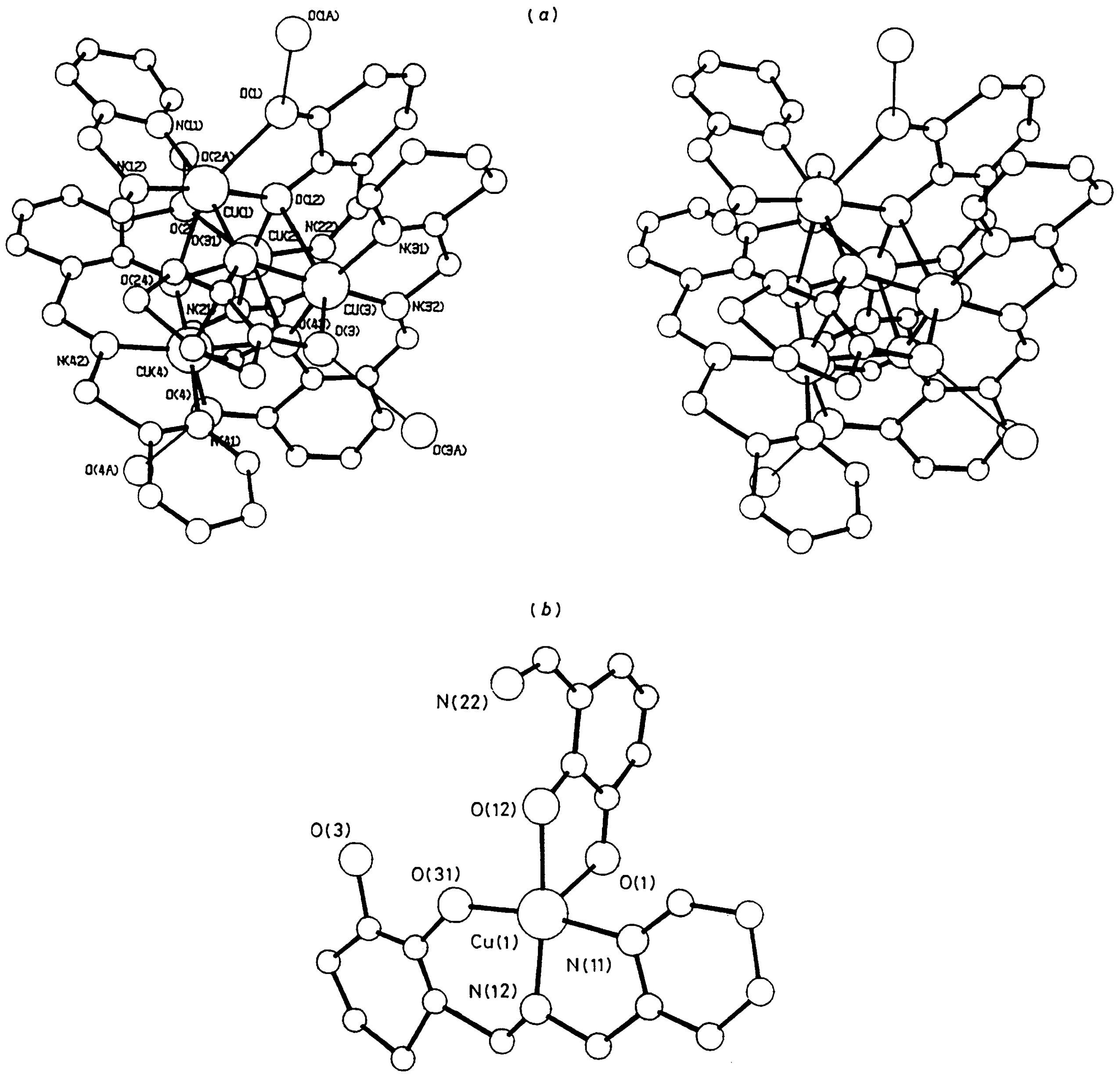

Figure 2. Structure of compound (**1**): (*a*) a stereoview of the whole cluster; (*b*) co-ordination sphere of Cu(1) showing the respective arrangements of the three ligands around the metal

around Cu(1) approaches a trigonal bipyramid; the axis of the pyramid is occupied by the catechol oxygen O(2) and the pyridine nitrogen N(2). The corresponding angle O(2)Cu(1)N(2) 177.1° slightly departs from the theoretical value of 180°. More deformation occurs within the basal plane constituted by the imine nitrogen N(1) and two acetato oxygens O(3) and O(5): the related angles present a 10° deviation from the ideal 120°. The symmetry around Cu(2) is close to a square pyramid whose basal plane comprises three catechol oxygens and an acetate oxygen O(4), and the apical position is occupied by a fifth oxygen atom, O(6), from a different acetate; Cu(2) is displaced from the O(4)O(2)O(1)O(1′) plane by 0.28 Å toward O(6). By symmetry, the Cu(2)O(1)Cu(2′)O(1′) parallelogram is perfectly planar; the Cu(2)O(1)Cu(2′) angle is 103.1°. The Cu(2)Cu(2′) distance within the inter-unit Cu_2O_2 bridge is shorter than the Cu(1)Cu(2) distance within the binuclear unit (3.053 *vs.* 3.303 Å). The three-atom acetate bridges undoubtedly open the CuOCu angle [Cu(1)O(2)Cu(2) 115°] and push the metals apart by comparison with the single-atom phenoxo-type bridge. Finally, mean C–O and C–C bond lengths are 1.33 and 1.41 Å, respectively, which supports the copper(II)–catecholate formulation *vs.* the copper(I)–semiquinone alternative.[1,16]

Owing to the poor quality of the crystals it has not been possible, despite thorough attempts, to refine the structure of compound (**1**) so as to get very precise structural data, as explained in the Experimental section. Nevertheless, during this study, a clear picture of the complex has emerged which is quite sufficient to explain its magnetic behaviour. This structure is illustrated in Figure 2. The complex is tetranuclear and adopts a distorted cubane arrangement, the four copper atoms being bridged by four catecholate oxygens. This kind of Cu_4O_4 array is quite common for copper alkoxides.[19] All copper atoms are in a very distorted octahedral environment which involves donor atoms from three different ligand molecules. A sketch of the copper co-ordination sphere is shown in Figure 2(*b*) and Tables 3 and 4 list the atomic co-ordinates and essential bond

Table 3. Atomic positional parameters (× 10^4) with e.s.d.s for compound (**1**)

Atom	*x*	*y*	*z*
Cu(1)	0.217 9(4)	0.182 3(4)	0.100 0(6)
Cu(2)	0.323 8(4)	0.136 1(4)	0.275 4(6)
Cu(3)	0.166 6(4)	0.074 9(4)	0.246 0(6)
Cu(4)	0.286 2(4)	0.029 4(4)	0.113 1(6)
O(1)	0.143(2)	0.245(2)	0.170(3)
O(2)	0.390(2)	0.206(2)	0.223(3)
O(3)	0.111(2)	0.002(2)	0.165(3)
O(4)	0.356(2)	−0.027(2)	0.200(3)
O(12)	0.240(2)	0.180(2)	0.248(3)
O(24)	0.326(2)	0.109(2)	0.134(3)
O(31)	0.174(2)	0.101(2)	0.106(3)
O(43)	0.253(2)	0.033(2)	0.253(3)
N(11)	0.264(3)	0.260(3)	0.072(4)
N(12)	0.207(2)	0.176(3)	−0.032(3)
N(21)	0.407(3)	0.094(3)	0.325(4)
N(22)	0.314(2)	0.147(2)	0.408(3)
N(31)	0.082(3)	0.113(3)	0.270(4)
N(32)	0.170(2)	0.056(2)	0.374(3)
N(41)	0.241(2)	−0.053(2)	0.076(3)
N(42)	0.307(3)	0.038(3)	−0.015(4)
C(11)	0.233(4)	0.232(4)	−0.077(6)
C(12)	0.173(4)	0.145(4)	−0.085(5)
C(21)	0.362(5)	0.118(5)	0.467(7)
C(22)	0.275(3)	0.184(4)	0.442(5)
C(31)	0.118(4)	0.089(4)	0.421(6)
C(32)	0.205(3)	0.028(3)	0.430(5)
C(41)	0.277(4)	−0.014(5)	−0.077(6)
C(42)	0.345(4)	0.076(4)	−0.066(6)
C(111)	0.295(3)	0.299(3)	0.125(5)
C(112)	0.331(3)	0.353(3)	0.115(4)
C(113)	0.337(3)	0.361(4)	0.019(5)
C(114)	0.309(3)	0.322(4)	−0.044(5)
C(115)	0.275(3)	0.273(3)	−0.014(5)
C(121)	0.161(3)	0.248(3)	0.257(4)
C(122)	0.117(3)	0.283(3)	0.319(4)
C(123)	0.125(3)	0.290(3)	0.402(5)
C(124)	0.180(4)	0.260(4)	0.443(5)
C(125)	0.221(3)	0.218(3)	0.397(5)
C(126)	0.206(3)	0.213(3)	0.304(4)
C(211)	0.452(4)	0.078(4)	0.278(6)
C(212)	0.517(4)	0.060(4)	0.327(6)
C(213)	0.519(6)	0.055(6)	0.418(9)
C(214)	0.474(4)	0.073(4)	0.465(5)
C(215)	0.414(4)	0.099(4)	0.407(5)
C(221)	0.405(3)	0.191(3)	0.117(5)
C(222)	0.449(4)	0.227(4)	0.064(6)
C(223)	0.457(4)	0.211(4)	−0.020(5)
C(224)	0.425(4)	0.165(4)	−0.059(5)
C(225)	0.376(4)	0.131(4)	−0.005(6)
C(226)	0.364(3)	0.142(4)	0.076(5)
C(311)	0.048(4)	0.137(4)	0.205(5)
C(312)	−0.020(4)	0.164(4)	0.207(5)
C(313)	−0.035(4)	0.158(4)	0.301(6)
C(314)	−0.001(3)	0.146(4)	0.369(5)
C(315)	0.069(3)	0.118(3)	0.343(5)
C(321)	0.110(3)	0.014(3)	0.063(4)
C(322)	0.073(3)	−0.028(3)	0.008(4)
C(323)	0.076(4)	−0.002(4)	−0.079(5)
C(324)	0.111(4)	0.048(4)	−0.127(6)
C(325)	0.142(3)	0.081(3)	−0.036(5)
C(326)	0.143(3)	0.062(3)	0.041(4)
C(411)	0.211(3)	−0.096(3)	0.124(5)
C(412)	0.178(3)	−0.148(3)	0.095(4)
C(413)	0.181(4)	−0.160(4)	0.004(6)
C(414)	0.210(4)	−0.123(4)	−0.044(6)
C(415)	0.242(3)	−0.061(3)	−0.006(4)
C(421)	0.338(4)	−0.037(5)	0.294(6)
C(422)	0.364(5)	−0.077(5)	0.371(7)
C(423)	0.339(4)	−0.084(4)	0.450(5)
C(424)	0.288(4)	−0.048(4)	0.464(5)
C(425)	0.255(3)	−0.005(3)	0.404(4)
C(426)	0.277(4)	−0.004(4)	0.323(6)
O(1A)	0.031(3)	0.287(3)	0.084(4)
O(2A)	0.473(3)	0.287(3)	0.309(5)
O(3A)	0.042(3)	−0.086(3)	0.240(4)
O(4A)	0.467(3)	−0.077(4)	0.164(5)

lengths and angles around the copper atoms. The two oxygens play drastically different roles: the internal one which belongs to the Cu_4O_4 core is triply bridging and is involved twice as an equatorial and once as an axial ligand, while the external one is only implied as a terminal axial ligand. This particular arrangement gives rise to a new chelating mode involving both equatorial and axial bonding which is unprecedented in copper catecholate chemistry. It is less stable than the purely equatorial one since it is broken in solution (see below). As a consequence in this compound the copper ions are bound in the lateral site of the ligands.

Another point of interest is the overall arrangement of the whole cluster: the ligand molecules are parallel to a face of the cube, and they occur as two pairs [Cu(1), Cu(4) and Cu(2), Cu(3)] of parallel molecules perpendicular to the other pair. The copper–copper distances reflect this arrangement: long separations are observed within the two pairs (average Cu ··· Cu distance 3.5 Å), whilst short distances occur between coppers of different pairs (average 3.3 Å). These distances are consistent with the axial–equatorial bridging pattern within the cube. The long intra-pair distances are probably caused by the steric repulsion of the ligand molecules. This interpretation is supported by the structures of two tetrameric complexes of 3,5-di-t-butylcatecholate (dtbc) recently reported by Olmstead *et al.*[20] The copper derivative $[Cu_4(dtbc)_4(py)_4]$ (py = pyridine) presents the same arrangement of the catechol planes as found in (**1**) but it does not exhibit a cubane structure;[20a] due to the presence of the bulky t-butyl groups, the shortest Cu ··· O distance achievable between two such planes is 3.175 Å. This distance is too long for the cube being formed. The cubane core Co_4O_4 is formed, however, in $[Co_4(dtbc)_4(thf)_{5.5}]$ (thf = tetrahydrofuran);[20b] distortions of the cubane structure and of the octahedral cobalt co-ordination sphere help to accommodate the presence of the bulky substituents allowing an angle of about 50° between the catechol planes. Along these lines, it seems reasonable to argue that in complex (**1**) the intrinsic repulsion of the ligand molecules is not large enough to hinder the formation of the cubane structure, but that this repulsion is reflected in the corresponding Cu–O bond lengths being the longest ones in the cube.

Magnetic Susceptibility.—Figure 3 illustrates the temperature dependence of the magnetic susceptibilities of the two tetranuclear derivatives (**1**) and (**4**) in the form of the χT *vs.* T curve over the range 6—300 K. The curve for (**1**) exhibits the shape characteristic of antiferromagnetically coupled tetranuclear copper clusters[19] with a decrease of χT from a high-temperature value of 1.2 $cm^3 mol^{-1}$ to a value close to 0 at low temperature indicating that all four copper atoms are coupled. The distortion of the cluster from the pure cubane symmetry allows us to distinguish two types of interactions between the copper atoms: the first involves copper atoms of different pairs which are separated by a short distance (3.3 Å) and, in spite of small structural differences, we have assumed that these *interpair* exchange constants were identical ($J = J_{12} = J_{13} = J_{24} = J_{34}$). The second one occurs between copper atoms of

Table 4. Selected bond lengths and interatomic distances (Å) and bond angles (°) with e.s.d.s for compound (**1**)

Cu(1) ··· Cu(2)	3.351(11)	Cu(4)–O(24)	1.90(4)
Cu(1) ··· Cu(3)	3.315(12)	Cu(4)–O(43)	2.16(4)
Cu(1) ··· Cu(4)	3.541(12)	Cu(4)–N(41)	2.03(5)
Cu(2) ··· Cu(3)	3.471(11)	Cu(4)–N(42)	1.92(6)
Cu(2) ··· Cu(4)	3.301(12)	O(1) ··· O(1A)	2.66(7)
Cu(3) ··· Cu(4)	3.345(12)	O(2) ··· O(2A)	2.66(9)
Cu(1)–O(1)	2.32(5)	O(3) ··· O(3A)	2.63(7)
Cu(1)–O(12)	2.14(4)	O(4) ··· O(4A)	2.58(9)
Cu(1)–O(31)	1.97(4)	Cu(1)–O(31)	1.97(4)
Cu(1)–N(11)	1.97(5)	Cu(1)–N(11)	1.97(5)
Cu(1)–N(12)	1.90(5)	Cu(1)–N(12)	1.90(5)
Cu(2)–O(2)	2.18(5)	Cu(2)–O(12)	1.97(4)
Cu(2)–O(12)	1.97(4)	Cu(2)–N(21)	2.01(6)
Cu(2)–O(24)	2.11(4)	Cu(2)–N(22)	1.94(5)
Cu(2)–N(21)	2.01(6)	Cu(3)–O(31)	2.09(4)
Cu(2)–N(22)	1.94(5)	Cu(3)–O(43)	1.98(4)
Cu(3)–O(3)	2.20(4)	Cu(3)–N(31)	1.96(6)
Cu(3)–O(31)	2.09(4)	Cu(3)–N(32)	1.88(5)
Cu(3)–O(43)	1.98(4)	Cu(4)–O(24)	1.90(4)
Cu(3)–N(31)	1.96(6)	Cu(4)–N(41)	2.03(5)
Cu(3)–N(32)	1.88(5)	Cu(4)–N(42)	1.92(6)
Cu(4)–O(4)	2.20(5)		
Cu(2)–Cu(1)–Cu(3)	62.8(3)	O(2)–Cu(2)–O(24)	78(2)
Cu(2)–Cu(1)–Cu(4)	57.2(2)	O(2)–Cu(2)–N(21)	84(2)
Cu(3)–Cu(1)–Cu(4)	58.3(2)	O(2)–Cu(2)–N(22)	111(2)
Cu(1)–Cu(2)–Cu(3)	58.1(2)	O(12)–Cu(2)–O(24)	91(2)
Cu(1)–Cu(2)–Cu(4)	64.3(3)	O(12)–Cu(2)–N(21)	171(2)
Cu(3)–Cu(2)–Cu(4)	59.1(2)	O(12)–Cu(2)–N(22)	89(2)
Cu(1)–Cu(3)–Cu(2)	59.1(2)	O(24)–Cu(2)–N(21)	98(2)
Cu(1)–Cu(3)–Cu(4)	64.2(3)	O(24)–Cu(2)–N(22)	170(2)
Cu(2)–Cu(3)–Cu(4)	57.9(2)	N(21)–Cu(2)–N(22)	81(2)
Cu(1)–Cu(4)–Cu(2)	58.5(3)	O(3)–Cu(3)–O(31)	75(2)
Cu(1)–Cu(4)–Cu(3)	57.5(2)	O(3)–Cu(3)–O(43)	98(2)
Cu(2)–Cu(4)–Cu(3)	63.0(3)	O(3)–Cu(3)–N(31)	87(2)
O(1)–Cu(1)–O(12)	72(2)	O(3)–Cu(3)–N(32)	110(2)
O(1)–Cu(1)–O(31)	99(2)	O(31)–Cu(3)–O(43)	93(2)
O(1)–Cu(1)–N(11)	87(2)	O(31)–Cu(3)–N(31)	100(2)
O(1)–Cu(1)–N(12)	116(2)	O(31)–Cu(3)–N(32)	173(2)
O(12)–Cu(1)–O(31)	90(2)	O(43)–Cu(3)–N(31)	167(2)
O(12)–Cu(1)–N(11)	99(2)	O(43)–Cu(3)–N(32)	83(2)
O(12)–Cu(1)–N(12)	173(2)	N(31)–Cu(3)–N(32)	84(2)
O(31)–Cu(1)–N(11)	170(2)	O(24)–Cu(4)–N(41)	173(2)
O(31)–Cu(1)–N(12)	88(2)	O(24)–Cu(4)–N(42)	87(2)
N(11)–Cu(1)–N(12)	83(2)	N(41)–Cu(4)–N(42)	87(2)
O(2)–Cu(2)–O(12)	99(2)	Cu(1)–O(31)–Cu(3)	110(2)

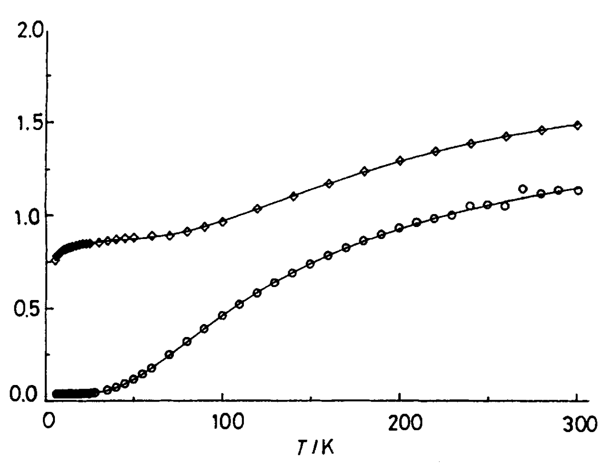

Figure 3. Temperature dependence of the product of the molar magnetic susceptibility and the temperature for compounds (**1**) (○) and (**4**) (◇). Solid lines are theoretical curves (see text).

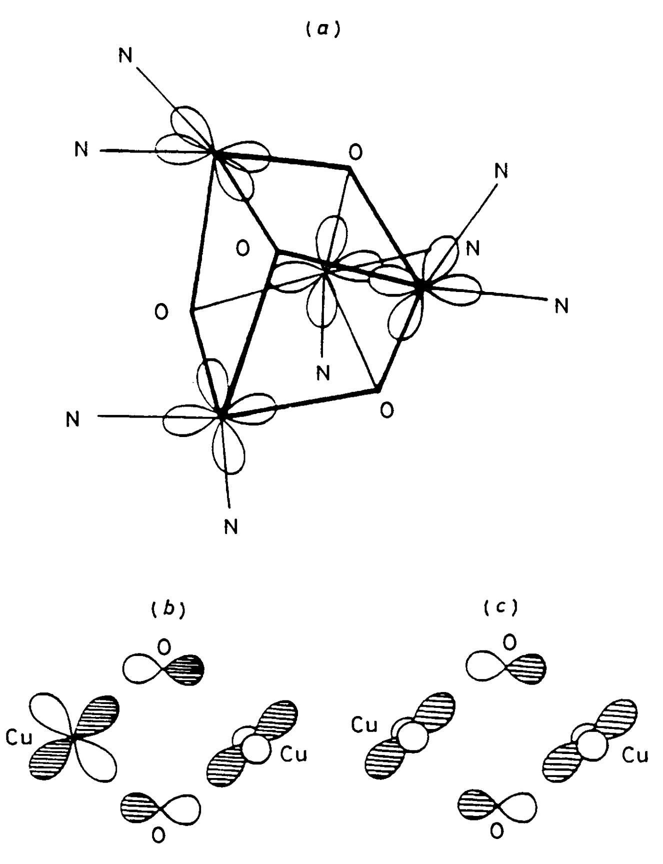

Figure 4.(*a*) Metallic contributions to the magnetic orbitals within the tetranuclear cluster (*b*) Equatorial–equatorial and axial–equatorial inter-pair interactions (*J* exchange integral) (*c*) Axial–equatorial intra-pair interactions (*J*′ exchange integral)

the same pairs at a longer distance (3.5 Å), and again these *intrapair* interactions have been considered identical ($J' = J_{14} = J_{23}$). The resulting situation is depicted by the Hamiltonian (1). Calculations were performed as usual[21] while

$$\mathscr{H} = -2J(\vec{S}_1\cdot\vec{S}_2 + \vec{S}_1\cdot\vec{S}_3 + \vec{S}_2\cdot\vec{S}_4 + \vec{S}_3\cdot\vec{S}_4) - 2J'(\vec{S}_1\cdot\vec{S}_4 + \vec{S}_2\cdot\vec{S}_3) \quad (1)$$

taking into account the presence of a Curie-behaved contaminant. In a first approximation, the intrapair exchange constant has been assumed negligible ($J' = 0$). This model satisfactorily accounts for the experimental data (Figure 3) and produce the following 'best-fit' values: $g = 2.02$, $J = -65\ \text{cm}^{-1}$, $2N\alpha = 1.50 \times 10^{-4}$, $g_m = 2.17$, and $P_m = 0.079$. It is to be noted that taking into account the two neglected exchange integrals does not lead to a significant improvement of the fit. These results can be easily rationalized by considering [Figure 4(*a*)] the orientation of the metallic component ($d_{x^2-y^2}$) of the magnetic orbitals deduced from the structural analysis presented above. It appears that both of the oxygen bridges of coppers of the same pairs (1,4 and 2,3) are axial to one metal atom and equatorial to the other; this gives rise to the overall situation shown in Figure 4(*c*). It is clear that this arrangement does not lead to a strong overlap between the metallic orbitals on any bridging atom, and, therefore, the interaction cannot be important. The interpair interaction, on the other hand, implies two different types of bridges: one of the axial–equatorial type as above, but, also, one of the equatorial–equatorial type. As illustrated in Figure 4(*b*), the latter combination produces a significant overlap on one bridging oxygen, thus providing a

Table 5. Spectroscopic and conductivity data in methanol solution

Compound	Λ[a]/ µS cm^{-1}	Electronic absorptions, λ/nm (ε/dm^3 mol^{-1} cm^{-1})		$g_{\parallel}$	A[b]	$g_{\perp}$
(1)	85	630 (127)	390 (2 945)	2.237	188	2.047
(2)	67	625 (140)	385 (4 550)	2.257	183	2.049
(3)	26		300 (12 450)			
(4)	58	730(120)	387 (2 360)			

[a] For a millimolar solution. [b] In Gauss (10^{-4} T).

Table 6. Electrochemical potentials (in V *vs.* s.c.e.) in dimethylformamide solution[a]

Compound	E_{p_c}	E_{p_a}	$E_{\text{p}_\text{c}}{}^2$	$E_{\text{p}_\text{a}}{}^2$	$E_{\text{p}_\text{c}}{}^3$	$E_{\text{p}_\text{a}}{}^3$
H_2L^1[b]			−0.37	0.66 −0.22[c]	0.16	1.04 0.68[c]
(1)	−0.57[d] 0.12[e]	−0.44[d] 0.25[e]	−0.34	0.56	0.20	0.88
(2)	−0.54	0.14	−0.34	0.70		
(3)	−0.40	−0.12	0.20	0.70		
(4)	−0.34	−0.14	0.28	0.80		

[a] Supporting electrolyte, tetrabutylammonium tetrafluoroborate (0.1 mol dm^{-3}); platinum electrode; sweep rate 3 V min^{-1}. [b] In acetonitrile. [c] In the presence of 2 equivalents of tetrabutylammonium hydroxide. [d] Referred to as couple A in the text and Figure 5. [e] Referred to as couple B in the text and Figure 5.

pathway to the magnetic interaction. The lack of precise structural data prevents a detailed discussion of the strength of this interaction.

As shown in Figure 3, the χT values of complex **(4)** decrease with temperature until about 60 K where a plateau is reached. This behaviour reveals that the magnetism of the tetranuclear complex is reduced by an antiferromagnetic interaction until it reaches the value expected for two independent spins $S = \frac{1}{2}$. Owing to the structural results, this situation corresponds to the two external coppers Cu(1) and Cu(1′) being isolated from the pair of central ones, Cu(2), Cu(2′), thus giving a pair of independent spins and a binuclear unit. Such a situation is described by equation (2). Fitting the curve with the variables

$$\chi_{\text{calc.}} = \frac{N\beta^2 g_1{}^2}{2k(T-\theta)} + \frac{2N\beta^2 g_2{}^2}{3kT}\left(1 + \frac{1}{3}e^{-2J/kT}\right) + 2N\alpha \quad (2)$$

g_1, θ, g_2, J, and $2N\alpha$ gives the following results: $g_1 = 2.16$, $\theta = -0.75$ K, $g_2 = 2.18$, $-2J = 259$ cm^{-1}, and $2\text{N}\alpha = 2.4 \times 10^{-4}$ cm^3 mol^{-1}. The most surprising observation is the absence of coupling within the basic binuclear unit Cu(1)Cu(2) while a significant interaction occurs between two coppers from different entities, Cu(2)Cu(2′). These results can be explained through consideration of the symmetries of the magnetic orbitals of the two different copper sites. Actually, Cu(2) is in a tetragonal environment which implies that the odd electron resides in the $d_{x^2-y^2}$ orbital pointing toward the four oxygen atoms of the basal plane. Accordingly, a good overlap results on the oxygen bridge O(1) and O(1′), and a significant interaction is expected as observed. All things being equal, this interaction is weaker than the ones observed for dihydroxy[22] and dialkoxy[23] bridged dicopper complexes; this is in line with the reduced electronegativity of the catechol oxygen with respect to the hydroxy and alkoxy ones.[24] The magnetic orbital of Cu(1) is d_{z^2} pointing toward O(2) and N(2) because of the trigonal-bipyramidal environment of the metal. Therefore, at first glance, an interaction is expected between Cu(1) and Cu(2) since their respective magnetic orbitals would overlap on the catechol oxygen O(2) and the angle Cu(1)O(2)Cu(2) is obtuse enough (115°) for such an interaction to be significant. In fact there is no significant coupling as evidenced by the value of the Weiss constant ($|\theta| < 1$ K). We think that two reasons may be advanced for this. First, Kida and co-workers[25a] and Reed and co-workers[25b] have shown that μ-1,3-acetate and alkoxide bridges are *countercomplementary*. However, this effect is not likely to be important here since both of the acetates occupy equatorial positions of the trigonal bipyramid and do not interact strongly with the magnetic orbital (d_{z^2}) of Cu(1). The second reason may be found in the non-planarity of the system. Actually, the N(2)Cu(1)O(2) axis makes an angle of 129° with the Cu(2) basal plane [O(1), O(1′), O(4), O(2)]. This situation is reminiscent of the folding observed for a dihydroxy-bridged dicopper complex[26] which exhibits an antiferromagnetic coupling weaker than anticipated from the CuOCu angle. The theory[27] predicts that this effect is maximum for a dihedral angle of 130°. Since the observed dihedral angle (129°) approaches this optimum value it is reasonable to think that this folding is responsible for the lack of interaction between the two coppers.

The magnetic properties of compound **(3)** can be analysed as those of **(4)**; however, the resulting exchange is much lower ($J = -50$ cm^{-1}). Complex **(2)** behaves as a binuclear complex with a singlet–triplet separation of -7 cm^{-1}. In the absence of structural data, further discussion of the magnetic properties of both compounds is precluded.

Solution Studies.—Spectroscopy. Although tetranuclear in the solid state complex **(1)** is probably mononuclear in solution since in methanol it behaves as a 1:1 electrolyte. U.v.–visible and e.s.r. data (Table 5) show that it is in a tetragonal environment ($g_{\parallel} > g_{\perp}$). Moreover its spectral similarity with the salicylaldehyde analogue[30] (λ 635 and 378 nm, $g_{\parallel} = 2.243$, $g_{\perp} = 2.059$) is in agreement with the co-ordination of the copper in the lateral site as found in the solid state. Similar results are obtained with complex **(2)** except for a lower value of the conductivity which indicates that, in solution, **(2)** retains the dimeric structure found in the solid state. Electrochemical experiments in dimethylformamide (dmf) point also to a dimeric structure. A low value of the conductivity is noted again for **(4)** in methanol solution, which suggests only the partial release of an acetate ion. It is likely that in solution the tetranuclear assembly is broken since solvent molecules can complete the co-ordination sphere of Cu(1). In agreement with the presence of the trigonal copper, in this compound, the *d–d* transitions move to lower energy (Table 5).

Electrochemistry. The ligand H_2L^1 and the copper complexes have been studied in acetonitrile and in dmf, respectively, at a platinum electrode with tetrabutylammonium tetrafluoroborate as supporting electrolyte. Table 6 lists the electrochemical data for all compounds; the acetate complexes **(3)** and **(4)** give poorly defined waves and have not been studied further.

Cyclic voltammetry shows that H_2L^1 undergoes two electrochemically irreversible oxidations [Figure 5(*a*)]. An additional reduction peak is observed at $E_{\text{p}_\text{c}} = -1.6$ V *vs.* s.c.e. with no oxidation counterpart which probably corresponds to the reduction of the catechol protons.[29] In the presence of 2 equivalents of tetrabutylammonium hydroxide this peak disappears and the two oxidation peaks move to less positive potentials ($E_{\text{p}_\text{a}}{}^2 = -0.22$ and $E_{\text{p}_\text{a}}{}^3 = 0.68$ V *vs.* s.c.e. Accordingly, it is likely that the two oxidative processes at positive potentials correspond to the successive one-electron oxidations of the catechol moiety: Catechol $\xrightarrow[-\text{H}^+]{-e^-}$ semiquinone $\xrightarrow[-\text{H}^+]{-e^-}$ quinone.

Complex **(1)** exhibits an electrochemical behaviour classical for copper compounds, with a stereochemical change accompanying the electron transfer to the copper(II) ion.[30] As

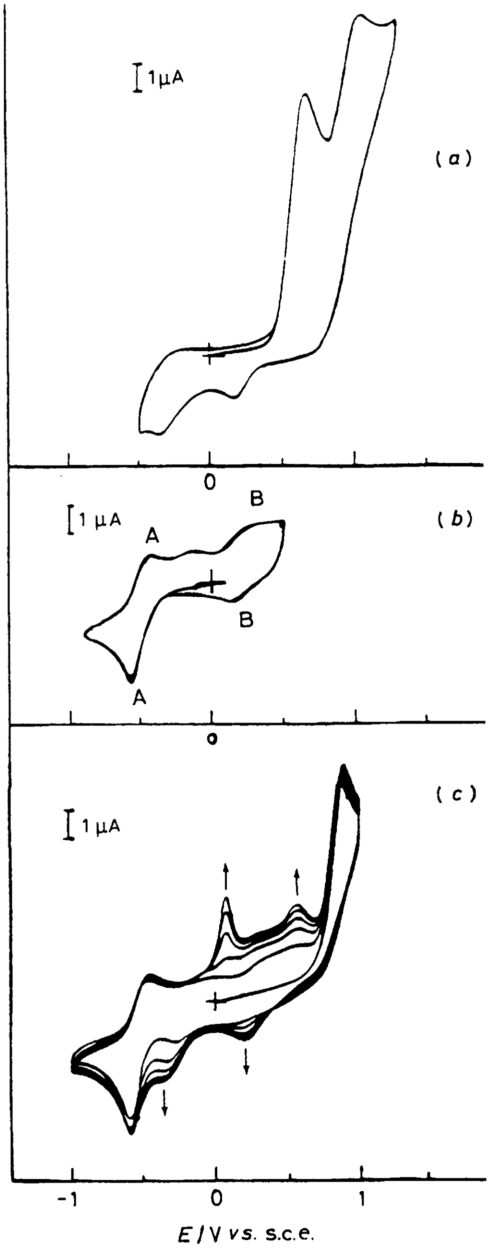

Figure 5. Cyclic voltammetry of (*a*) H_2L^1 in acetonitrile, (*b*) and (*c*) complex (**1**) in the reduction and oxidation domains, respectively, in dimethylformamide

shown in Figure 5(*b*), after reduction of the tetragonal copper(II) complex (couple A), the stereochemical distortion favouring the copper(I) state causes the appearance of a new cyclic voltammetry response (couple B) at more positive potentials. Exhaustive reduction at −0.7 V and reoxidation at 0.55 V *vs.* s.c.e. each consume 1 F mol^{-1}. As judged by u.v. and e.s.r. spectroscopies as well as electrochemical techniques, the solution is recovered unchanged after a reduction–oxidation cycle. The electroactivity of the catechol ligand is clearly observable at more positive potentials [Figure 5(*c*)]. Cycling of the solution in the −1 to +1 V *vs.* s.c.e. range reveals that the ligand oxidation at E_{p_a} = 0.88 V is at least partly reversible (chemically) since the copper(II)–copper(I) couple is not much affected. However, the peak characteristic of free Cu^{2+} (E_{p_a} = 0.12 V) appears after a few cycles and indicates the release of copper from the ligand. Simultaneously, the electrochemical response of the free ligand appears. Metal release after oxidation to the quinone has been observed previously for copper[12] and iron[31] catecholates. On the other hand, electrolysis at 0.9 V *vs.* s.c.e. requires four electrons per mole and produces a solution whose electrochemical response is identical to that of copper(II) nitrate. This observation is consistent with the overall oxidation of the ligand resulting in cleavage of the benzene ring and release of the metal ion.

In contradistinction with (**1**), the chloride (**2**) exhibits in cyclic voltammetry two reduction peaks at E_{p_c} = −0.54 and −1.05 V *vs.* s.c.e. The first reduction is electrochemically irreversible ($E_{p_a}{}^1$ = 0.14 V) and electrolysis at −0.7 V consumes 0.5 electron per copper. The resulting solution shows a frozen-state e.s.r. spectrum [$g_{\parallel}$ = 2.228, $A_{\parallel}$ = 167 G (1.67 × 10^{-2} T), $g_{\perp}$ = 2.050] characteristic of a tetragonal site and very similar to that of the starting compound (**2**) (Table 5). Reoxidation at 0.4 V *vs.* s.c.e. requires 0.5 electron per copper and regenerates the starting solution as deduced from u.v. and e.s.r. spectroscopies and electrochemical techniques. Exhaustive electrolysis at −1.4 V consumes 1.5 electrons per copper and leads to copper deposition on the platinum electrode and release of the free ligand. These observations are consistent with the mechanism depicted in the Scheme. Reduction of (**2**) which is a dimer leads to a mixed-valence compound. Reduction of the latter gives a dicopper(I) species which disproportionates.

$$[Cu^{II}Cu^{II}(HL^1)_2Cl_2] + e^- \rightleftharpoons [Cu^{II}Cu^{I}(HL^1)_2Cl_2]^-$$

$$[Cu^{II}Cu^{I}(HL^1)_2Cl_2]^- + e^- \rightleftharpoons [Cu^{I}Cu^{I}(HL^1)_2Cl_2]^{2-}$$

$$2[Cu^{I}Cu^{I}(HL^1)_2Cl_2]^{2-} \rightleftharpoons 2Cu^0 + 2HL^{1-} + 2Cl^- + [Cu^{II}Cu^{II}(HL^1)_2Cl_2]$$

Scheme.

This study has shown that it is possible to divert a catechol from its most common chelating bonding mode[7] through the use of a complexing side arm. The unsymmetrical bonding is revealed by *X*-ray diffraction as well as spectroscopic studies. Nevertheless, the chelating bonding mode may occur in addition to the lateral one as in complex (**4**) and in a pentanuclear copper(II) cluster.[18] This is in line with the high affinity of copper(II) for chelating catechols. Consistently, the same trend is observed for iron(III) for which monodentate catecholates have been isolated in addition to the usual bidentate derivatives.[31b] Also, it is noteworthy that in (**1**) a new chelating equatorial–axial mode is revealed whose stability is lower since it is cleaved in solution. The electrochemical studies have shown that stable copper(I) catecholates are attainable without using soft coligands such as phosphines.[9,16] This behaviour * departs from that observed for the salicylaldehyde analogues in which disproportionation of copper(I) occurs.[31] This difference emphasizes the fact that very subtle factors govern the stability of copper(I). On the other hand, oxidation of the catechol moiety eventually results in the release of the copper atom. This points to the necessity of stronger complexing arms to hold the copper ions if one wants the catechol ligand to assist the metal in the electron transfers.[32]

Experimental

General Methods.—All chemicals and solvents were reagent grade and used as received except for electrochemical measurements (see below). N.m.r. and e.s.r. spectra were

---

* Copper(I) disproportionation is observed for (**1**) in wet solvents; if the solvent is rigorously dried, (**1**) can be reduced and reoxidized without disproportionation.

recorded with a Brucker AC 200 and a Varian E 104 spectrometer, respectively, u.v.–visible and i.r. spectra with Beckman Acta MVI and IR 4250 spectrophotometers, respectively. Magnetic susceptibility studies were done as described previously[18] except that the function (3) was

$$R = \Sigma(\chi_{\text{obs.}} - \chi_{\text{calc.}})^2/N\Sigma(\chi_{\text{obs.}})^2 \qquad (3)$$

employed in the least-squares minimization where N is the number of measurements. $R = 4.7 \times 10^{-6}$ [(**1**)], 5.3×10^{-6} [(**2**)], 1.5×10^{-5} [(**3**)], and 3.2×10^{-7} [(**4**)].

Electrochemical experiments were performed in dmf as described previously.[33] Potentials are referenced to the saturated calomel electrode; under the conditions used in the present study the potential of the ferrocene–ferrocenium couple was 0.47 V *vs.* s.c.e.

Syntheses.—3-[(2′-*Pyridyl*)*methyliminomethyl*]*benzene*-1,2-*diol* (H_2L^1). To 2,3-dihydroxybenzaldehyde (691 mg, 5 mmol) in absolute ethanol (80 cm^3) was added slowly a solution of 2-aminomethylpyridine (540 mg, 5 mmol) in absolute ethanol (50 cm^3). The reaction mixture was heated to 50 °C for 30 min while stirring and, after cooling to room temperature, the solvent was evaporated. The resulting oil was diluted with absolute ethanol (10 cm^3) and left at −20 °C for several hours. Upon filtration (H_2L^1) was obtained as fine yellow needles (877 mg, 78%), m.p. 136—137 °C (Found: C, 68.6; H, 5.2; N, 12.2; O, 14.0%; $[M + H]^+$, m/z 229. $C_{13}H_{12}N_2O_2$ requires C, 68.4; H, 5.3; N, 12.25; O, 14.0%; M 228); $\nu_{\text{max.}}$(CN) 1 630 cm^{-1} (KBr). N.m.r. ($CDCl_3$, from $SiMe_4$): ^1H, δ 8.6 (1 H, d, H^{13}), 8.4 (1 H, s, H^7), 7.7 (1 H, t, H^{11}), 7.35 (1 H, d, H^{10}), 7.25 (1 H, d, H^{12}), 7.0—6.85 (2 H, dd, $H^3 + H^5$), 6.7 (1 H, t, H^4), and 4.9 (1 H, s, H^8); ^{13}C, δ 166.6 (C^7), 157.3 (C^9), 152.5 (C^1), 149.7 (C^{13}), 145.9 (C^2), 137.0 (C^{11}), 122.6 (C^6), 122.3 and 122.0 (C^{10}, C^{12}), 117.9, 117.4, and 116.9 (C^3, C^4, C^5), and 63.1 p.p.m. (C^8).

3-[2′-(2″-*pyridylethyl*)*iminomethyl*]*benzene*-1,2-*diol* (H_2L^2). To 2,3-dihydroxybenzaldehyde (2.76 g, 2×10^{-2} mol) in absolute ethanol (100 cm^3) was added slowly while stirring a solution of 2-(2′aminoethyl)pyridine (2.44 g, 2×10^{-2} mol) in absolute ethanol (100 cm^3). The reaction mixture was stirred and heated to 50 °C for 1 h. After cooling to room temperature the solvent was stripped off. The resulting brown oil was dried in vacuum at 50 °C; H_2L^2 precipitated as a yellow powder (4.17 g, 86%), m.p. 116 °C (Found: C, 69.2; H, 5.9; N, 11.5; O, 13.4%; $[M + H]^+$, m/z 243. $C_{14}H_{14}N_2O_2$ requires C, 69.4; H, 5.8; N, 11.55; O, 13.2%); $\nu_{\text{max.}}$(CN) 1 630 cm^{-1} (KBr). N.m.r. ($CDCl_3$, from $SiMe_4$): ^1H, δ 8.6 (1 H, d, H^{14}), 8.1 (1 H, s, H^7), 7.6 (1 H, t, H^{12}), 7.15 (1 H, d, H^{11}), 7.10 (1 H, d, H^{13}), 6.85 and 6.65 (2 H, dd + dd, $H^3 + H^5$), 6.55 (1 H, t, H^4), 4.0 (1 H, t, H^8), and 3.2 (1 H, t, H^9); ^{13}C, δ 165.1 (C^7), 158.4 (C^{10}), 155.5 (C^1), 149.6 (C^{14}), 146.5 (C^2), 136.6 (C^{12}), 123.8 (C^6), 122.0 and 121.8 (C^{11}, C^{13}), 116.9, 116.5, and 116.2 (C^3, C^4, C^5), 55.9 (C^8), and 39.0 p.p.m. (C^9).

$[\{Cu(HL^1)(NO_3)\}_4]$ (**1**). A filtered solution of copper nitrate (1.5 g, 6 mmol) in absolute ethanol (90 cm^3) was added to a solution of H_2L^1 prepared as described above. The reaction mixture was stirred and heated to reflux for 30 min. After cooling to room temperature, evaporation of the solvent over several days furnished fine green crystals (Found: C, 42.2; H, 3.2; Cu, 17.0; N, 11.3. $C_{13}H_{13}CuN_3O_6$ requires C, 42.1; H, 3.55; Cu, 17.15; N, 11.35%).

$[\{Cu(HL^1)Cl\}_2]\cdot 2H_2O$ (**2**). A filtered solution of copper chloride (852 mg, 5 mmol) in absolute ethanol (20 cm^3) was added at 50 °C to a solution of H_2L^1 prepared as described above. A green precipitate formed immediately. After cooling to room temperature, the reaction mixture was stirred for 2 h and then filtered; 1.24 g (72%) of complex (**2**) were thus obtained. The powder was dissolved in methanol (1 l) and after slow evaporation of about one third of the solvent the solution was kept at −20 °C for several days. Fine deep green needles separated (Found: C, 45.6; H, 3.7; Cu, 18.7; N, 8.4. $C_{13}H_{13}ClCuN_2O_3$ requires C, 45.35; H, 3.8; Cu, 18.45; N, 8.15%).

$[\{Cu_2L^1(CH_3CO_2)_2\}_2]\cdot 3H_2O$ (**3**). A filtered solution of copper acetate (2 g, 2×10^{-2} mol) in absolute ethanol (80 cm^3) was added at 50 °C to a solution of H_2L^1 prepared as described above. Heating was maintained for 15 min and after cooling to −20 °C for 2 h a brown powder separated off. This powder was solubilized in methanol and precipitation was effected by slow evaporation and sequential additions of acetone. This procedure furnished complex (**3**) as a brown powder (1.33 g, 53%) (Found: C, 41.0; H, 3.8; Cu, 25.5; N, 5.6. $C_{17}H_{18}Cu_2O_{7.5}$ requires C, 40.9; H, 3.65; Cu, 25.15; N, 5.7%).

$[\{Cu_2L^2(CH_3CO_2)_2\}_2]\cdot H_2O$ (**4**). A solution of 2-(2′-aminoethyl)pyridine (1.22 g, 1×10^{-2} mol) in absolute ethanol (100 cm^3) was added slowly to a solution of 2,3-dihydroxybenzaldehyde (1.38 g, 10^{-2} mol) in absolute ethanol (100 cm^3). The pale yellow reaction mixture was heated to 50 °C for 30 min. A solution of copper acetate (4 g, 2×10^{-2} mol) in absolute ethanol (200 cm^3) was then added and the reaction mixture was heated to reflux for 15 min. Upon cooling to room temperature a brown powder formed which was collected by filtration and then washed with acetonitrile. Upon dissolution in methanol and cooling to −20 °C pale brown plates crystallized out after a few days (Found: C, 43.7; H, 3.8; Cu, 24.5; N, 5.5. $C_{18}H_{19}Cu_2O_{6.5}$ requires C, 43.7; H, 3.85; Cu, 25.7; N, 5.65%).

X-Ray Data Collections and Structure Determinations.—Data were collected with an Enraf–Nonius CAD4 diffractometer using graphite-monochromated Mo-K_α radiation and operating in the ω—2θ mode with scan width = 0.7 + 0.35 tanθ and a scan speed of 2° min^{-1}. Complex (**4**) crystallizes in the space group $P\bar{1}$ with $Z = 2$, $a = 8.365(2)$, $b = 9.667(1)$, $c = 12.556(1)$ Å, $\alpha = 98.40(2)$, $\beta = 103.97(2)$, $\gamma = 94.26(2)°$, $U = 968.4(5)$ Å^3, $D_c = 1.696$ g cm^{-3}, μ(Mo-K_α) = 22.4 cm^{-1}, λ(Mo-K_α) = 0.710 69 Å, and $F(000) = 476$. Intensities of 4 075 reflections with $(\sin\theta)/\lambda < 0.62$ were measured, among which a total of 1 038 with $I < 3.0\sigma(I)$ were classified as unobserved. The structure was solved by the heavy-atom technique and refined by full-matrix least squares to $R = 0.044$. Non-hydrogen atoms were allocated anisotropic thermal parameters, hydrogen atoms fixed thermal parameters, $B = 5.0$ Å^2. Omitting the water oxygen atom O(7) results in a 3.1% increase in the R factor. The weighting scheme was $w^{-1} = [\sigma(F^2) + (0.05F)^2 + 5.0]$. The high B factor is indicative of disorder, but the occupancy was not refined. Table 1 lists the atomic positional parameters.

Complex (**1**) crystallizes in the space group $P2_1/n$, with $a = 20.47(5)$, $b = 21.27(5)$, $c = 14.31(7)$ Å, $\beta = 93.93(7)$, $U = 6\,219(10)$ Å^3, $Z = 4$, $D_c = 1.306$ g cm^{-3}, μ(Mo-K_α) = 14.1 cm^{-1}, λ(Mo-K_α) = 0.710 69 Å, and $F(000) = 2\,512$. 8 130 Reflections ($hk \pm l$; $1 < \theta < 22°$) were collected, yielding 7 347 unique reflections with 1 250 having $I > 3\sigma(I)$. No decay was observed in the crystal during the course of data collection. The structure was solved by the heavy-atom method. The extremely small crystal size (dimensions 0.08 × 0.08 × 0.03 mm; attempts to grow larger crystals were unsuccessful) resulted in a very poor set of data. Even increasing the counting time to a maximum of 300 s failed to improve the situation dramatically. Initially, the positions of three copper atoms were determined, the fourth being found from a subsequent Fourier map. Numerous structure-factor/Fourier calculations eventually allowed a partial structure consisting of 52 atoms to be produced. Subsequent isotropic refinement (R = 0.275) allowed the remainder of the structure to be found which was further refined using only anisotropic thermal parameters for the copper atoms ($R = 0.174$). Introduction of a suitable weighting scheme, $w = 1/[\sigma(F^2) + (XF)^2 + Y]$ with initial values of X and Y of 0.05 and 5.0, and the inclusion of all reflections for which $I > \sigma(I)$ allowed refinement to continue although numerous isotropic thermal parameters fell to unacceptably low values. A reappraisal of the weighting scheme coefficients ($X = 0.03$, $Y = 3.0$) allowed refinement to continue with a subsequent difference map locating four peaks assumed to be water molecules (based on geometry). The refinement was eventually terminated at $R = 0.125$, $R' = 0.159$ with an estimated standard deviation of unit weight of 1.29 for 1 240 reflections. Some bond lengths and angles showed large deviations from the accepted values together with large standard deviations, a not surprising result considering the small ratio of observations to parameters. No improvement was obtained by reinstating those reflections for which $\sigma(I) < I < 3\sigma(I)$ into the refinement and it is almost certain that poor data quality from the extremely small crystal is the reason for this. Table 3 lists the atomic positional parameters.

All calculations were performed on a DEC PDP 11/73 computer using the SDP Plus V 1.1a system of crystallographic programs.[34]

Additional material available from the Cambridge Crystallographic Data Centre comprises thermal parameters and remaining bond lengths and angles.

References

1 C. G. Pierpont and R. M. Buchanan, *Coord. Chem. Rev.*, 1981, **38**, 45.

2 M. M. Rogic, M. D. Swerdloff, and T. R. Demmin, in 'Copper Coordination Chemistry: Biochemical and Inorganic Perspectives,' eds. K. D Karlin and J. Zubieta, Adenine Press, Albany, 1983, pp. 259–280.

3 B. Reinhammar and B. G. Malmström, in 'Copper Proteins,' ed. T. G. Spiro, Wiley, New York, 1981, ch. 3, pp. 109—149; B. Reinhammar, in 'Copper Proteins and Copper Enzymes,' ed. R. Lontie, CRC Press, Boca Raton, 1984, vol. 3, ch. 1, pp. 1—35.

4 K. N. Raymond and C. J. Carrano, *Acc. Chem. Res.*, 1979, **12**, 183.

5 K. Lerch, in 'Metal Ions in Biological Systems,' ed. H. Sigel, Marcel Dekker, New York, 1981, vol. 13, ch. 5, pp. 143–186; L. Que, *Struct. Bonding (Berlin)*, 1980, **40**, 39; J. J. Villafranca, in 'Copper Proteins,' ed. T. G. Spiro, Wiley, New York, 1981, ch. 7, pp, 263—290.

6 C. A. Tyson and A. E. Martell, *J. Am. Chem. Soc.*, 1968, **90**, 3379.

7 R. Griesser and H. Sigel, *Inorg. Chem.*, 1970, **9**, 1238; P. R. Huber, R. Griesser, and H. Sigel, *ibid.*, 1971, **10**, 945; F. A. Walker, H. Sigel, and D. B. McCormick, *ibid.*, 1972, **11**, 2756; H. Sigel, P. R. Huber, R. Griesser, and B. Priss, *ibid.*, 1973, **12**, 1198; B. E. Fischer and H. Sigel, *ibid.*, 1979, **18**, 425.

8 D. G. Brown, J. T. Reinprecht, and G. C. Vogel, *Inorg. Nucl. Chem. Lett.*, 1976, **12**, 399; D. G. Brown, L. Beckmann, C. H. Ashby, G. C. Vogel, and J. T. Reinprecht, *Tetrahedron Lett.*, 1977, 1363; D. G. Brown and G. C. Vogel, *Inorg. Chem.*, 1978, **17**, 1367; D. G. Brown and W. J. Hughes, *Z. Naturforsch., Teil B*, 1979, **34**, 1408; D. G. Brown, W. J. Hughes, and G. Knerr, *Inorg. Chim. Acta*, 1980, **46**, 123.

9 V. A. Muraev, V. K. Cherkasov, G. A. Abakumov, and G. A. Razuvaev, *Dokl. Akad. Nauk. SSR*, 1977, **236**, 620; G. A. Razuvaev, V. K. Cherkasov, and G. A. Abakumov, *J. Organomet. Chem.*, 1981, **160**, 361; G. A. Abakumov, A. V. Lobanov, V. K. Cherkasov, and G. A. Razuvaev, *Inorg. Chim. Acta*, 1981, **49**, 135.

10 W. L. Kwik and K. P. Ang, *Aust. J. Chem.*, 1978, **31**, 459.

11 E. Balogh-Hergovich and G. Speier, *Inorg. Chim. Acta*, 1985, **108**, 59; G. Speier and Z. Tyeklar, in 'Biological and Inorganic Copper Chemistry,' eds. K. D. Karlin and J. Zubieta, Adenine Press, Albany, 1984, vol. 2, pp. 91—100.

12 S. Harmalker, S. E. Jones, and D. T. Sawyer, *Inorg. Chem.*, 1983, **22**, 2790.

13 K. Andra and F. Fleischer, *Z. Anorg. Allg. Chem.*, 1982, **485**, 210.

14 J. S. Thompson and J. C. Calabrese, *Inorg. Chem.*, 1985, **24**, 3167; *J. Am. Chem. Soc.*, 1986, **108**, 1903.

15 K. D. Karlin, Y. Gultneh, T. Nicholson, and J. Zubieta, *Inorg. Chem.*, 1985, **24**, 3725.

16 R. M. Buchanan, C. Wilson-Blumenberg, C. Trapp, S. K. Larsen, D, L. Greene, and C. G. Pierpont, *Inorg. Chem.*, 1986, **25**, 3070.

17 E. Gojon, S. J. Greaves, J. M. Latour, D. C. Povey, and G. W. Smith, *Inorg. Chem.*, 1987, **26**, 1457.

18 E. Gojon, J. Gaillard, J. M. Latour, and J. Laugier, *Inorg. Chem.*, 1987, **26**, 2046.

19 W. Haase, *J. Mol. Catal.*, 1984, **23**, 331.

20 (*a*) M. M. Olmstead, P. P. Power, G. Speier, and Z. Tyeklar, *Polyhedron*, 1988, **7**, 609; (*b*) M. M. Omstead, P. P. Power, and G. A. Sigel, *Inorg. Chem.*, 1988, **27**, 580.

21 P. H. Fries and E. Belorizky, *New. J. Chem.*, 1987, **11**, 271; E. Belorizky, P. H. Fries, E. Gojon, and J. M. Latour, *Mol. Phys.*, 1987, **61**, 661.

22 V. H. Crawford, H. W. Richardson, J. R. Wasson, D. J. Hodgson, and W. E. Hatfield, *Inorg. Chem.*, 1976, **25**, 2107.

23 L. Merz and W. Haase, *J. Chem. Soc., Dalton Trans.*, 1980, 875.

24 P. J. Hay, J. C. Thibeault, and R. Hoffmann, *J. Am. Chem. Soc.*, 1975, **97**, 4884.

25 (*a*) Y. Nishida, M. Takeuchi, K. Takahashi, and S. Kida, *Chem. Lett.*, 1985, 631; (*b*) V. McKee, M. Zvagulis, and C. A. Reed, *Inorg. Chem.*, 1985, **25**, 2914.

26 M. F. Charlot, O. Kahn, S. Jeannin, and Y. Jeannin, *Inorg. Chem.*, 1980, **19**, 1410.

27 O. Khan and M. F. Charlot, *Nouv. J. Chim.*, 1980, **4**, 567.

28 J. M. Latour, G. A. Leonard, D. Limosin, D. C. Povey, and S. S. Tandon, in 'Biological and Inorganic Copper Chemistry,' eds. K. D. Karlin and J. Zubieta, Adenine Press, Albany, 1985, vol. 2, pp. 221—230.

29 M. D. Stallings, M. M. Morrison, and D. T. Sawyer, *Inorg. Chem.*, 1981, **20**, 2655.

30 W. Mazurek, A. M. Bond, M. J. O'Connor, and A. G. Wedd, *Inorg. Chem.*, 1986, **25**, 906.

31 (*a*) L. Que, R. C. Kolanczyk, and L. S. White, *J. Am. Chem. Soc.*, 1987, **109**, 5373; (*b*) R. H. Heistand, A. L. Roe, and L. Que, *Inorg. Chem.*, 1982, **21**, 676.

32 E. Gojon, P. Dubourdeaux, N. Gon, and J. M. Latour, *New. J. Chem.*, 1988, **12**, 931.

33 N. A. Bailey, D. E. Fenton, J. Lay, P. B. Roberts, J. M. Latour, and D. Limosin, *J. Chem. Soc., Dalton Trans.*, 1986, 2681.

34 B. A. Frenz and Associates, Enraf-Nonius Structure Determination Package, SDP Users Guide, version 1.1a, Delft, 1983.

Received 13*th March* 1989, *revised manuscript received* 8*th December* 1989; *Paper* 9/01083A